

Phase diagram of Hubbard-Holstein model on 4-leg tube system at quarter-filling

Sahinur Reja¹, Satoshi Nishimoto^{2,3}

¹*Physics Department, Indiana University Bloomington, USA 47405*

²*Department of Physics, TU Dresden, 01069 Dresden, Germany and*

³*IFW Dresden, Helmholtzstrae 20, 01069 Dresden, Germany*

(Dated: August 27, 2018)

We derive an effective electronic Hamiltonian for square lattice Hubbard-Holstein model (HHM) in the strong electron-electron (e-e) and electron-phonon (e-ph) coupling regime and under non-adiabatic conditions ($t/\omega_0 \leq 1$), t and ω_0 being the electron hopping and phonon frequency respectively. Using Density Matrix Renormalization Group method, we simulate this effective electronic model on 4-Leg cylinder system at quarter-filling and present a phase diagram in $g-U$ plane where g and U are being the e-ph coupling constant and Hubbard on-site interaction respectively. For larger g , we find cluster of spins i.e. phase separation (PS) gives way to a charge density wave (CDW) phase made of NN singlets which abruptly goes to another CDW phase as we increase U . But for smaller g , we find a metallic phase sandwiched between PS and singlet CDW phase. This phase is characterized by vanishing charge gap but finite spin gap – suggesting a singlet superconducting phase.

PACS numbers: 71.10.Fd, 74.20.-z, 71.45.Lr, 71.38.-k

I. INTRODUCTION

More than one type of interactions typically manifests a variety of phases such as diagonal long range orders [such as charge density wave (CDW) and spin density wave (SDW)] and off-diagonal long range orders (such as superfluid and superconducting states) of which some co-operate and some compete. The study of coexistence and competition between these electronic phases is a subject of immense ongoing focus. In particular, the coexistence of CDW and superconductivity/superfluidity in layered dichalcogenides (e.g., 2H-TaSe₂, 2H-TaS₂, and NbSe₂)¹, helium-4², bismuthates (e.g., BaBiO₃ doped with K or P)³, quarter-filled organic materials^{4,5}, non-iron based pnictides (e.g., SrPt₂As₂)⁶, quasi-one-dimensional (1D) trichalcogenide NbSe₃⁷ and doped spin ladder cuprate Sr₁₄Cu₂₄O₄₁⁸, and recently in optical lattice system with effective long-range interactions⁹ etc.

Electron-phonon (e-ph) coupling along with usual electron-electron (e-e) interaction plays an important role in condensed matter systems such as cuprates^{10,11} and manganites^{12–14} and molecular solids such as fullerenes¹⁵. The interplay of e-e and e-ph interactions in these correlated systems gives rise to the competition/coexistence of various phase such as superconductivity, CDW, SDW etc.

The simplest model to study the co-occurring effects of e-e and e-ph interactions is the following well known Hubbard-Holstein model (HHM)¹⁶

$$H_{hh} = -t \sum_{j,\delta,\sigma} \left(c_{j\sigma}^\dagger c_{j+\delta,\sigma} + \text{H.c.} \right) + \omega_0 \sum_j a_j^\dagger a_j + g\omega_0 \sum_{j\sigma} n_{j\sigma} (a_j + a_j^\dagger) + U \sum_j n_{j\uparrow} n_{j\downarrow}, \quad (1)$$

where $c_{j\sigma}^\dagger$ is the fermionic creation operator for itinerant spin- σ electrons at site j with hopping integral t and

number operator $n_{j\sigma} \equiv c_{j\sigma}^\dagger c_{j\sigma}$. Here $\delta = (\hat{x}, \hat{y})$ with unit lattice parameter represents the nearest neighbors for square lattice which we consider for our calculations; a_j^\dagger is the corresponding bosonic creation operator characterized by a dispersionless phonon frequency ω_0 , with U and g representing the strengths of onsite e-e and e-ph interactions respectively.

The Hubbard-Holstein model has been extensively studied (in one-, two-, and infinite-dimensions and at various fillings) by employing various approaches such as exact diagonalization^{17–19}, density matrix renormalization group (DMRG)^{20,21}, quantum Monte Carlo (QMC)^{22–27}, dynamical mean field theory (DMFT)^{28–36}, semi-analytical slave boson approximations^{37–41}, large-N expansion⁴², variational methods based on Lang-Firsov transformation^{43,44}, Gutzwiller approximation^{45,46}, and cluster approximation⁴⁷.

However, the study of the subtle interplay of e-e and e-ph interaction effects in low-dimensional systems, such as conjugated polymers, charge transfer salts, inorganic spin-Peierls compounds, halogen-bridged transition metal complexes, ferroelectric perovskites, or organic superconductors^{48–51}, has attracted much attention. Apart from the superconductors, e-ph coupling in quasi-1D materials sometimes can drive the electrons to be insulating with a CDW by Peierls transition.

In our earlier work^{16,52}, in strong e-e and e-ph coupling regime, we derived an effective electronic Hamiltonian using a controlled analytic approach that takes into account dynamical quantum phonons. It was shown that the e-ph interaction generates nearest-neighbor (NN) repulsion which competes with NN spin antiferromagnetic (AF) interactions produced by e-e interactions. This competition stabilizes a correlated NN singlet phase for intermediate e-e and e-ph coupling which was shown to be a superfluid at all fillings (less than one-half) other than one-third where it is a CDW.

In this paper, we study the HHM on a 4-Leg tube system at quarter-filling using DMRG method which is very effective in studying ground-state properties of quasi-1D systems with short-range interactions⁵³. We show that NN singlet phase we uncovered for 1D HHM model^{16,52} still survives, but these singlets arrange themselves to form a CDW at quarter filling with finite charge and spin gap. This phase is shown to be stabilized between phase separation at smaller U and a CDW phase at larger U . At smaller e-e and e-ph coupling, we find a metallic phase in the vicinity of NN singlet-CDW phase and phase separation with vanishing charge gap, but with finite spin gap – suggesting a singlet superconducting phase.

The paper is organized as follows: in Sec. II we briefly derive the effective electronic Hamiltonian and explain the various interaction terms and hopping terms. We also briefly mention the details of DMRG simulations. In Sec. III, we present a phase diagram in $g - U/t$ plane mentioning different stable phases. Next, in Sec. IV we describe how we determine the different phase boundaries using DMRG simulations. For this we calculate charge gap, spin gap and different order parameters to identify various phases. Finally we conclude in Sec V.

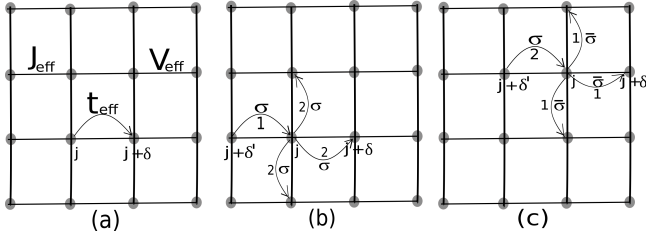


FIG. 1. (a) The effective NN terms in the hamiltonian, (b) Longer range σ -spin hopping from site $j+\delta'$ to site j and then to $j+\delta$ with $\delta, \delta' = \pm\hat{x}, \pm\hat{y}$ as appropriate to avoid double counting. Here as shown for the case of $\delta' = -\hat{x}$, we can have $\delta = \hat{x}, \pm\hat{y}$. (c) Similarly $\delta' = -\hat{x}$, and $\delta = \hat{x}, \pm\hat{y}$ for the $\sigma\bar{\sigma}$ pair hopping where $\bar{\sigma}$ -spin first hops from site j to $j+\delta$ and then opposite spin σ hops from site $j+\delta'$ to j . The number 1(2) represents the first(second) hopping process.

II. EFFECTIVE HHM HAMILTONIAN

Here we briefly outline the procedure to get the effective electronic Hubbard-Holstein Hamiltonian (with more details being provided in Ref. 16, 54, and 55). This approach involves a Lang-Firsov (LF) transformation⁵⁶ $H_{hh}^{LF} = e^T H_{hh} e^{-T}$ where $T = -g \sum_{j\sigma} n_{j\sigma} (a_j - a_j^\dagger)$ and get the following LF transformed Hamiltonian:

$$H_{hh}^{LF} = -t \sum_{j\delta\sigma} (X_{j+\delta}^\dagger c_{j+\delta,\sigma}^\dagger c_{j\sigma} X_j + \text{H.c.}) + \omega_0 \sum_j a_j^\dagger a_j - g^2 \omega_0 \sum_j n_j + (U - 2g^2 \omega_0) \sum_j n_{j\uparrow} n_{j\downarrow}, \quad (2)$$

where $X_j = e^{g(a_j - a_j^\dagger)}$ and $n_j = n_{j\uparrow} + n_{j\downarrow}$. Next, we express as follows our LF transformed Hamiltonian in terms of the composite fermionic operator $d_{j\sigma}^\dagger \equiv c_{j\sigma}^\dagger X_j^\dagger$:

$$H_{hh}^{LF} = -t \sum_{j\delta\sigma} (d_{j+\delta,\sigma}^\dagger d_{j\sigma} + \text{H.c.}) + \omega_0 \sum_j a_j^\dagger a_j + (U - 2g^2 \omega_0) \sum_j n_{j\uparrow}^\dagger n_{j\downarrow}^\dagger - g^2 \omega_0 \sum_j (n_{j\uparrow}^\dagger + n_{j\downarrow}^\dagger), \quad (3)$$

where $n_{j\sigma}^\dagger = d_{j\sigma}^\dagger d_{j\sigma}$. The last term is a constant polaronic energy and can be dropped. So Eq. (3) essentially represents the Hubbard Model for composite fermions with Hubbard interaction $U_{eff} = (U - 2g^2 \omega_0)$. The renormalization of Hubbard U by e-ph coupling has been recently observed in layered dichalcogenide 1T-TaS₂⁵⁷. In the limit of large U_{eff}/t , using standard treatment involving a canonical (Hubbard to $t - J$) transformation, we get the following effective Hamiltonian for the small parameter t/U_{eff} ⁵⁸⁻⁶⁰:

$$H_{t-J} = P_s \left[-t \sum_{j\delta} (d_{j+\delta,\sigma}^\dagger d_{j\sigma} + \text{H.c.}) + \omega_0 \sum_j a_j^\dagger a_j + J \sum_{j\delta} \left(\vec{S}_j \cdot \vec{S}_{j+\delta} - \frac{n_j^d n_{j+\delta}^d}{4} \right) \right] P_s \quad (4)$$

where $n_j^d = n_{j\uparrow}^d + n_{j\downarrow}^d$, $J = \frac{4t^2}{U_{eff}}$, \vec{S}_j is the spin operator for a spin 1/2 fermion at site j , and P_s is the single-occupancy-subspace projection operator. This is the $t - J$ Hamiltonian for the composite fermionic operators $d_{j\sigma}$.

In terms of original operators $c_{j\sigma}$, the effective $t - J$ Hamiltonian in Eq. (4) can be re-written as

$$H_{t-J} = H_0 + H_1, \quad (5)$$

where

$$H_0 = -te^{-g^2} \sum_{j\sigma} P_s (c_{j+\delta,\sigma}^\dagger c_{j\sigma} + \text{H.c.}) P_s + \omega_0 \sum_j a_j^\dagger a_j + J \sum_{j\delta} P_s \left(\vec{S}_j \cdot \vec{S}_{j+\delta} - \frac{n_j n_{j+1}}{4} \right) P_s \quad (6)$$

and

$$H_1 = -te^{-g^2} \sum_{j\sigma} P_s \left[c_{j+\delta,\sigma}^\dagger c_{j\sigma} (Y_+^{j\dagger} Y_-^j - 1) + \text{H.c.} \right] P_s. \quad (7)$$

Here we have rewritten the above Hamiltonian to separate into (i) the electronic part H_0 which is nothing but an effective $t - J$ model with reduced hopping (te^{-g^2}); and (ii) the remaining perturbative part H_1 which corresponds to the composite fermion terms containing the e-ph interaction with $Y_\pm^j \equiv e^{\pm g(a_{j+\delta} - a_j)}$.

After carrying out perturbation theory to second-order (as outlined in Ref. 16 and 52), with $t/(g\omega_0)$ as the small parameter⁵⁴), we get the following effective Hamiltonian:

$$H_{hh}^{eff} \cong -t_1 h_{t_1} + J h_S - V h_{nn} - t_2 h_{\sigma\sigma} - t_2 h_{\sigma\bar{\sigma}} \quad (8)$$

where

$$h_{t_1} = \sum_{j\delta\sigma} P_s \left(c_{j+\delta,\sigma}^\dagger c_{j\sigma} + \text{H.c.} \right) P_s, \quad (9)$$

$$h_S = \sum_{j\delta} P_s \left(\vec{S}_j \cdot \vec{S}_{j+\delta} - \frac{1}{4} n_j n_{j+\delta} \right) P_s, \quad (10)$$

$$h_{nn} = \sum_{j\delta\sigma} (1 - n_{j+\delta\bar{\sigma}})(1 - n_{j\bar{\sigma}})(n_{j\sigma} - n_{j+\delta\sigma})^2, \quad (11)$$

$$h_{\sigma\sigma} = \sum_{j\delta\delta'\sigma} (1 - n_{j+\delta',\bar{\sigma}})(1 - n_{j\bar{\sigma}})(1 - n_{j+\delta,\bar{\sigma}}) \times \left[c_{j+\delta,\sigma}^\dagger (1 - 2n_{j\sigma}) c_{j+\delta',\sigma} + \text{H.c.} \right], \quad (12)$$

$$h_{\sigma\bar{\sigma}} = \sum_{j\delta\delta'\sigma} (1 - n_{j+\delta,\bar{\sigma}})(1 - n_{j+\delta'\sigma}) \times \left[c_{j\sigma}^\dagger c_{j+\delta,\sigma} c_{j+\delta',\bar{\sigma}}^\dagger c_{j\bar{\sigma}} + \text{H.c.} \right], \quad (13)$$

The various coefficients are defined in terms of the system electron-phonon coupling g , the Hubbard interaction U , the hopping amplitude t , and the phonon frequency ω_0 as follows: $V \simeq t^2/2g^2\omega_0$, $J \equiv \frac{4t^2}{U-2g^2\omega_0}$, $t_1 \equiv te^{-g^2}$, and $t_2 \simeq t^2e^{-g^2}/g^2\omega_0$. Hereafter $t = 1$ is taken as unit of energy.

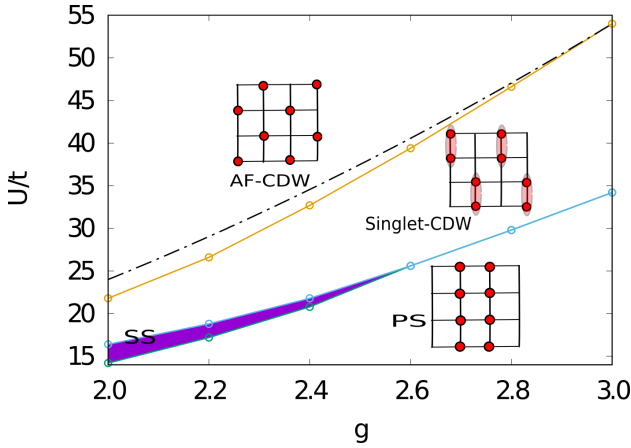


FIG. 2. Different phases in $g - U/t$ plane. Phase separation (PS) i.e. antiferromagnetic clustering of electrons at smaller U is broken to form insulating CDW made of NN singlets (two electron in shaded ellipse) i.e. singlet-CDW as we increase U . The breaking of singlet pairs happen with further increase in U to give AF-CDW as shown. At smaller g , a metallic phase sandwiched between PS and singlet-CDW is stabilized in narrow range of parameters. The dashed black line is an estimate of the boundary between singlet-CDW and AF-CDW when hopping is ignored (see main text).

Here we have the nearest neighbor parameter $\delta, \delta' = (\hat{x}, \hat{y})$ for each site j to cover the 2D square lattice for

the terms h_{t_1}, h_S, h_{nn} in effective Hamiltonian in Eq. 8. Here just to mention that the phonon averaging (upto 2nd order perturbation) introduces a dominant NN repulsion term h_{nn} which involves the electrons hopping to nearest neighbor sites and coming back. So this process prefers NN sites to be empty to avoid double occupancy and is basically a repulsion. Also this perturbation process includes longer range three site hopping process with further reduced amplitude t_2 . For each site j the next to NN (NNN) hopping terms $h_{\sigma\sigma}$ and $h_{\sigma\bar{\sigma}}$ have the sums over the parameters $(\delta, \delta') = (\pm\hat{x}, \pm\hat{y})$ to avoid double counting as described and shown in Fig.1.

To study the ground state properties of this model on quasi-1D systems, we simulate the model on 4-leg ladder system with periodic boundary condition in y -direction i.e., 4-leg tube system by using DMRG method⁵³. For different values of model parameters $(g, U/t)$, we simulate the system with different tube length and calculate the ground state energies and order parameters. These physical quantities are then used to extrapolate the results to thermodynamic limit by finite size scaling. We keep upto 8000 states of the density matrix to get the ground state energies with error $< 10^{-8}$.

III. PHASE DIAGRAM

Here we describe the different phases in $g - U/t$ plane at quarter-filling (one electron per two sites and equal number of up and down electrons) obtained by extensive DMRG simulation with $\omega_0/t = 1$. As mentioned above, we have two dominant interaction terms in Hamiltonian: the effective Heisenberg interaction $J/t \equiv \frac{4}{U-2g^2}$ which for a fixed g decreases with the increase in U and responsible for antiferromagnetic (AF) clustering of electrons i.e., phase separation (PS) and singlet pair formation; and an effective NN repulsion $V/t \simeq 1/(2g^2)$ which depends on g only and tries to break Phase separated cluster of spins and singlet pairs. As shown in Fig.2, for large g and smaller U , the system is phase separated i.e. clustering of spins happens due to large J . With increasing U , the cluster of spins breaks into singlet pairs (shaded pair of electrons) which at the commensurate quarter-filling are arranged in an insulating CDW state. We call it as singlet-CDW having structure factor peak at $S(\pi/2, \pi)$ or $S(\pi, \pi/2)$ depending on the orientation of the singlets. Further increase in U decreases J and the singlet pairs are broken to give another CDW phase as shown. The electrons are arranged in this phase to be AF order for smaller g to gain some kinetic energy due to NNN hopping terms. The transition between phases is found to be abrupt which seems to be reasonable due to the negligible contribution of effective hopping terms for larger g .

The situations is different for the case of smaller g and smaller U where NN hopping term $t_1 = e^{-g^2}$ can be effective. Along with the CDW phases at larger g , we find a narrow range of metallic phase sandwiched between PS

and singlet-CDW phase as shown as shaded area in Fig.2. This phase is characterized by the vanishing charge gap,

but with finite spin gap (singlet to triplet excitation). With increasing g , metallic phase is narrowed down and vanished at larger g .

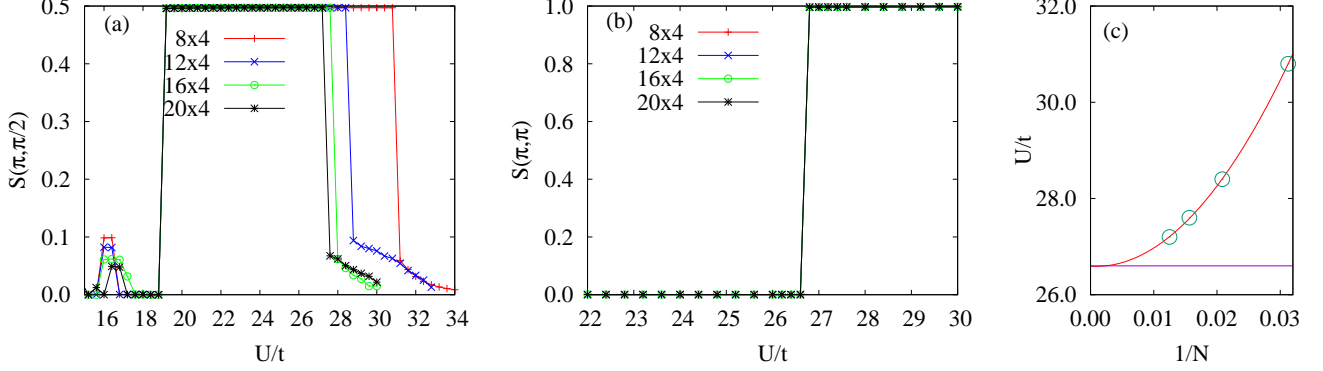


FIG. 3. The results are for $g = 2.2$: (a) The order parameter $S(\pi, \pi/2)$ i.e. the structure factor for singlet-CDW phase when the edge potential is arranged as $(\delta V, \delta V, -\delta V, -\delta V)$ and $(-\delta V, -\delta V, \delta V, \delta V)$ on two edges of the tube system to pick up the phase. (b) The order parameter $S(\pi/2, \pi/2)$ i.e. the structure factor for AF-CDW when a edge potential is arranged as $(-\delta V, \delta V, -\delta V, \delta V)$ and $(\delta V, -\delta V, \delta V, -\delta V)$ on two edges of the tube system to pick up the phase. (c) The finite size extrapolation to determine the phase boundary between singlet-CDW and AF-CDW.

IV. DETERMINATION OF PHASE BOUNDARIES

Here we discuss how we determine the phase boundaries in the phase diagram shown in Fig.2. The different insulating phases are characterized by the structure factor peak which is the Fourier transform of density-density correlations and is defined as:

$$S(k_x, k_y) = \frac{1}{N} \sum_{l_1, l_2} W(l_1, l_2) e^{-i(k_x l_1 + k_y l_2)} \quad (14)$$

where $W(l_1, l_2) = \langle n_{i,j} n_{i+l_1, j+l_2} \rangle$ is density-density correlation. For example, the singlet-CDW and AF-CDW phase can be captured by the structure factors $S(\pi, \pi/2)$ or $S(\pi/2, \pi/2)$ respectively. The metallic phase is detected by vanishing charge gap defined as $\Delta_c = (E(N+2, 0) + E(N-2, 0) - 2E(N, 0))/2$ with $E(N, S_z^T)$ being the energy for N number of electrons (equal up and down electrons) and total z component of spins $S_z^T = 0$. Also we confirm that metallic phase has non-zero spin gap Δ_s defined as $\Delta_s = E(N, 1) - E(N, 0)$. The phase separation has been captured by looking at the real space density profile obtained by DMRG simulations.

We simulate 4-leg tube systems of different sizes i.e., 8x4, 12x4, 16x4, 20x4 systems with periodic boundary condition in y-direction (i.e., 4-leg tube) and open boundary in tube direction. We study the quarter-filled system i.e., number of particle is $N/2$ (equal up and down electrons) where N is the total number of sites. The physical quantities calculated for different system sizes enable us

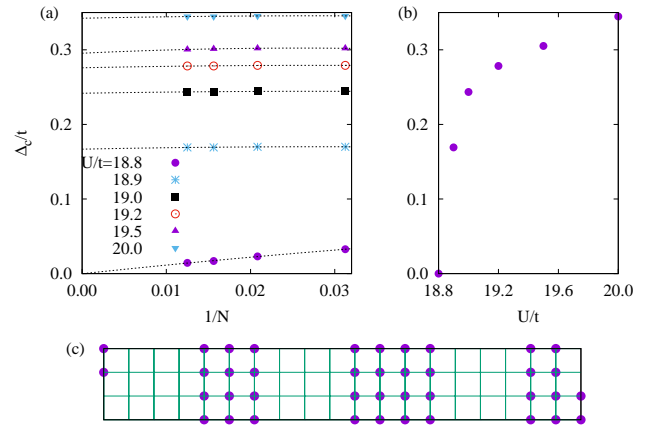


FIG. 4. For $g = 2.2$, (a) Typical extrapolation of charge gap (Δ_c) approached from singlet-CDW phase to metallic phase. (b) Δ_c as a function of U/t (c) Typical local density profile in phase separation.

to extrapolate the results to thermodynamic limit by finite size scaling analysis as described below.

A. Phase boundaries at smaller g

In our simulation, we pick up the different CDW phases mentioned in the phase diagram by adding onsite potential at two edges of the tube. This is used to reduce the edge effect for these insulating phases and does not affect

the results in thermodynamic limit.

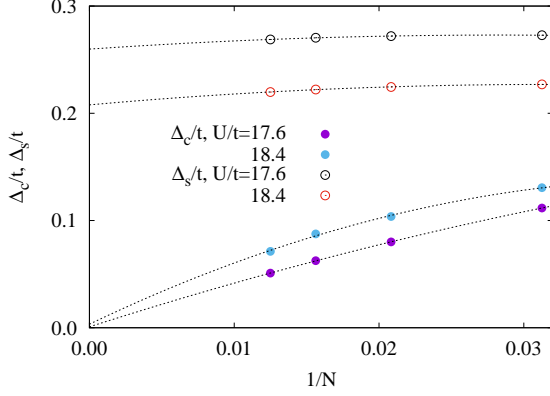


FIG. 5. For $g = 2.2$, typical extrapolation of charge gap (Δ_c) and spin gap (Δ_s) in the metallic phase.

So, we use edge potential as $(\delta V, \delta V, -\delta V, -\delta V)$ on one edge and $(-\delta V, -\delta V, \delta V, \delta V)$ on the other to pick up the singlet-CDW phase. Then we calculate the order parameter $S(\pi/2, \pi)$ for this phase in the intermediate region of the phase diagram. Note that the order parameter persists for arbitrary long system length and corresponds to long range singlet-CDW state. The results are shown for $g = 2.2$ in Fig.3(a). This shows finite size effect on singlet-CDW and AF-CDW phase boundary, but almost no effect on the boundary with PS phase. We also simulate the same systems after putting the edge potential as $(\delta V, -\delta V, \delta V, -\delta V)$ on one edge and $(-\delta V, \delta V, -\delta V, \delta V)$ on the other to settle the AF-CDW boundary from above. The order parameter in this case is $S(\pi/2, \pi/2)$ and is shown in Fig.3(b) to have no finite size effect. We then

extrapolate the two results which are shown to coincide to same U as shown in Fig.3(c)—suggesting a abrupt transition between singlet-CDW and AF-CDW. This transition can also be captured analytically ignoring the hopping contributions. The effective model contains J and V terms. So in singlet-CDW phase, the energy of a singlet corresponds to $-3J/4 + (2V - J/4)$ which becomes zero at the singlet-CDW to AF-CDW transition points. After writing these in terms of U and g , this gives the transition at $U/t \sim 6g^2$ which estimates the singlet-CDW to AF-CDW transition better at larger g (see Fig.2). Also, we want to point out that we calculate the expectation value of the singlet operator $(S_i^+ S_j^- + S_i^- S_j^+)$ for each bond connecting two NN sites i, j in singlet-CDW phase. This gives the value -1 (as it should be for a NN singlet pair between NN sites i, j) for each NN bond forming a NN singlet and 0 otherwise.

For smaller g , the NN hopping can be effective and we find that the breaking of cluster of spins at smaller U goes through a metallic phase before forming singlet-CDW phase. To find the metallic phase boundary with singlet-CDW, we calculate charge gap Δ_c in the singlet-CDW phase with the edge potential as mentioned above. As we decrease U , we see the extrapolated Δ_c goes to zero as shown in Fig.4(a) and (b). The metallic boundary with phase separation has been captured by investigating the local electron density profile obtained by the DMRG simulation. The typical density profile in PS is shown in Fig.4(c) where the filled circle size represents the total electron density. We also confirm the vanishing charge gap, but non-zero spin gap inside the metallic phase as shown in Fig.5. So this metallic phase is characterized as singlet superconducting (SS) phase as shown in Fig.2.

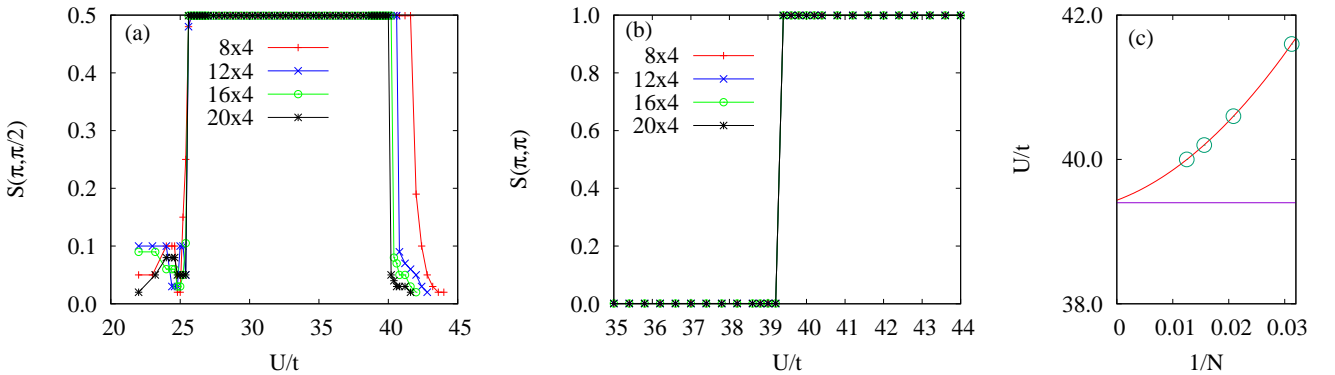


FIG. 6. Similar calculations for $g = 2.6$ as shown in Fig.3

B. Phase boundaries at larger g

Again we present the similar calculations for larger $g = 2.6$ to detect the phase boundaries. The results

are shown in Fig.6. We see similar behavior at larger U where the boundary approached from both CDW phases seems to be coinciding as shown in Fig.6(c). In contrast

to smaller g , we have not detected any metallic phase for $g = 2.6$ and larger. This seems to be reasonable because for larger g , the hopping terms become less effective. In Fig.7, the typical extrapolation of charge gap (Δ_c) around the singlet-CDW and PS boundary stays always finite. Although, a tendency to PS for smaller system gives slightly negative Δ_c/t , the 'normal' insulating state is restored for larger system sizes.

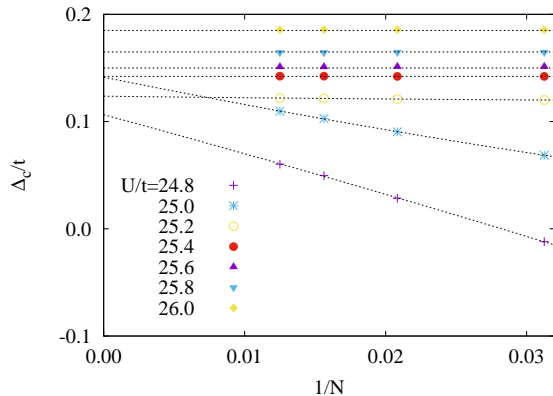


FIG. 7. For $g = 2.6$, typical extrapolation of charge gap (Δ_c) around the singlet-CDW and PS boundary

V. CONCLUSIONS

In both strong electron-electron and electron-phonon coupling regime, we derive an effective electronic Hamiltonian for two dimensional Hubbard-Holstein model by

averaging out phonon degrees of freedom within second order perturbation theory. Using density matrix renormalization group method, we simulate the effective electronic Hamiltonian on 4-leg tube systems to identify the different phases of the model in $g - U/t$ parameter space. The phase boundaries are captured by structure factor peak, charge gap and real space density profile obtained from DMRG simulations which are extrapolated to the thermodynamic limit. We show that for larger g , the system goes through the phase separation, singlet-CDW and AF-CDW phases respectively as we increase U/t . The phase transitions seems to be abrupt as the effective hopping is negligible for larger g . For smaller g , we also get the similar CDW phases (AF-CDW and singlet-CDW) at larger U/t . But for smaller U/t , the hopping of electrons can be effective which gives rise to a metallic phase sandwiched between singlet-CDW and phase separation. This phase is characterized by vanishing charge gap, but non-zero spin gap—suggesting a singlet superconducting phase. The phase diagram mostly contains the insulating phases. In particular, the exotic singlet-CDW phase might be relevant to CDW phases arising from the interplay of electron-electron and electron-phonon coupling and observed in layered dichalcogenide 1T-TaS₂⁵⁷.

VI. ACKNOWLEDGMENTS

S.R would like to thank Sudhakar Yarlagadda, Peter B. Littlewood and Herbert Fertig for stimulating discussions. We would like to thank U. Nitzsche for technical assistance. This work was supported by the NSF through Grant Nos. DMR-1506263 and DMR-1506460 and by SFB 1143 of the Deutsche Forschungsgemeinschaft. Computations were carried out on the ITF/IFW Dreden, Germany.

- ¹ For a review, see R. L. Withers and J. A. Wilson, J. Phys. C **19**, 4809 (1986).
- ² E. Kim and M. H. W. Chan, Nature **427**, 225 (2004); Science **305**, 1941 (2004).
- ³ S. H. Blanton, R. T. Collins, K. H. Kelleher, L. D. Rotter, and Z. Schlesinger, Phys. Rev. B **47**, 996 (1993).
- ⁴ H. Mori, I. Hirabayashi, S. Tanaka, T. Mori, Y. Maruyama, and H. Inokuchi, Solid State Commun. **80**, 411 (1991).
- ⁵ J. Merino and R. H. McKenzie, Phys. Rev. Lett. **87**, 237002 (2001).
- ⁶ K. Kudo, Y. Nishikubo, M. Nohara, J. Phys. Soc. Jpn. **79**, 123710 (2010).
- ⁷ W. W. Fuller, P. M. Chaikin, and N. P. Ong, Phys. Rev. B **24**, 1333 (1981).
- ⁸ A. Rusydi, W. Ku, B. Schulz, R. Rauer, I. Mahns, D. Qi, X. Gao, A. T. S. Wee, P. Abbamonte, H. Eisaki, Y. Fujimaki, S. Uchida, and M. Rübhausen, Phys. Rev. Lett. **105**, 026402 (2010); P. Abbamonte, G. Blumberg, A. Rusydi, A. Gozar, P. G. Evans, T. Siegrist, L. Venema, H. Eisaki, E. D. Isaacs, and G. A. Sawatzky, Nature (London) **431**, 1078 (2004).

- ⁹ R. Landig, L. Hruby, N. Dogra, M. Landini, R. Mottl, T. Donner, and T. Esslinger, Nature (London) **532**, 476 (2016).
- ¹⁰ A. Lanzara, P. V. Bogdanov, X. J. Zhou, S. A. Kellar, D. L. Feng, E. D. Lu, T. Yoshida, H. Eisaki, A. Fujimori, K. Kishio, J.-I. Shimoyama, T. Noda, S. Uchida, Z. Hussain, and Z. X. Shen, Nature (London) **412**, 510 (2001).
- ¹¹ G.-H. Gweon, T. Sasagawa, S. Y. Zhou, J. Graf, H. Takagi, D.-H. Lee, and A. Lanzara, Nature (London) **430**, 187 (2004).
- ¹² A. Lanzara, N. L. Saini, M. Brunelli, F. Natali, A. Bianconi, P. G. Radaelli, and S.-W. Cheong Phys. Rev. Lett. **81**, 878 (1998).
- ¹³ A. J. Millis, P. B. Littlewood, and B. I. Shraiman, Phys. Rev. Lett. **74**, 5144 (1995).
- ¹⁴ F. Massee, S. de Jong, Y. Huang, W. K. Siu, I. Santoso, A. Mans, A. T. Boothroyd, D. Prabhakaran, R. Follath, A. Varykhalov, L. Patthey, M. Shi, J. B. Goedkoop, and M. S. Golden, Nature Physics advance online publication, 11 September 2011, (DOI:10.1038/nphys2089).
- ¹⁵ O. Gunnarsson, Rev. Mod. Phys. **69**, 575 (1997).
- ¹⁶ Sahinur Reja, S. Yarlagadda, and P. B. Littlewood, Phys. Rev. B **84**, 085127 (2011).

- ¹⁷ A. Dobry, A. Greco, J. Lorenzana, and J. Riera, Phys. Rev. B **49**, 505 (1994).
- ¹⁸ A. Dobry, A. Greco, J. Lorenzana, J. Riera, and H. T. Diep, Europhys. Lett. **27**, 617 (1994).
- ¹⁹ B. Bäuml, G. Wellein, and H. Fehske, Phys. Rev. B **58**, 3663 (1998).
- ²⁰ M. Tezuka, R. Arita, and H. Aoki, Phys. Rev. B **76**, 155114 (2007).
- ²¹ Shigetoshi Sota and Takami Tohyama, Phys. Rev. B **82**, 195130 (2010).
- ²² J. E. Hirsch and E. Fradkin, Phys. Rev. B **27**, 4302 (1983).
- ²³ J. E. Hirsch, Phys. Rev. B **31**, 6022 (1985).
- ²⁴ E. Berger, P. Valášek, and W. von der Linden, Phys. Rev. B **52**, 4806 (1995).
- ²⁵ Z. B. Huang, W. Hanke, E. Arrigoni, and D. J. Scalapino, Phys. Rev. B **68**, 220507(R) (2003).
- ²⁶ R. P. Hardikar and R. T. Clay, Phys. Rev. B **75**, 245103 (2007).
- ²⁷ A. Macridin, G. A. Sawatzky, and M. Jarrell, Phys. Rev. B **69**, 245111 (2004).
- ²⁸ J. K. Freericks and M. Jarrell, Phys. Rev. Lett. **75**, 2570 (1995).
- ²⁹ M. Capone, G. Sangiovanni, C. Castellani, C. Di Castro, and M. Grilli, Phys. Rev. Lett. **92**, 106401 (2004).
- ³⁰ W. Koller, D. Meyer, Y. Ono, and A. C. Hewson, Europhys. Lett. **66**, 559 (2004).
- ³¹ W. Koller, D. Meyer, and A. C. Hewson, Phys. Rev. B **70**, 155103 (2004).
- ³² G. S. Jeon, T.-H. Park, J. H. Han, H. C. Lee, and H.-Y. Choi, Phys. Rev. B **70**, 125114 (2004).
- ³³ G. Sangiovanni, M. Capone, C. Castellani, and M. Grilli, Phys. Rev. Lett. **94**, 026401 (2005).
- ³⁴ G. Sangiovanni, M. Capone, and C. Castellani, Phys. Rev. B **73**, 165123 (2006).
- ³⁵ J. Bauer and A. C. Hewson Phys. Rev. B **81**, 235113 (2010).
- ³⁶ Johannes Bauer and Giorgio Sangiovanni, Phys. Rev. B **82**, 184535 (2010).
- ³⁷ M. Grilli and C. Castellani, Phys. Rev. B **50**, 16880 (1994).
- ³⁸ J. Keller, C. E. Leal, and F. Forsthofer, Physica B **206-207**, 739 (1995).
- ³⁹ E. Koch and R. Zeyher, Phys. Rev. B **70**, 094510 (2004).
- ⁴⁰ U. Trapper, H. Fehske, M. Deeg, and H. Buttner, Z. Phys. B: Condens. Matter **93**, 465 (1994).
- ⁴¹ C. A. Perroni, V. Cataudella, G. De Filippis, and V. Marigliano Ramaglia, Phys. Rev. B **71**, 113107 (2005).
- ⁴² R. Zeyher and M. L. Kulić, Phys. Rev. B **53**, 2850 (1996).
- ⁴³ Y. Takada and A. Chatterjee, Phys. Rev. B **67**, 081102 (2003).
- ⁴⁴ H. Fehske, D. Ihle, J. Loos, U. Trapper, and H. Buttner, Z. Phys. B: Condens. Matter **94**, 91 (1994).
- ⁴⁵ A. Di Ciolo, J. Lorenzana, M. Grilli, and G. Seibold, Phys. Rev. B **79**, 085101 (2009).
- ⁴⁶ P. Barone, R. Raimondi, M. Capone, C. Castellani, and M. Fabrizio, Phys. Rev. B **77**, 235115 (2008).
- ⁴⁷ Alexandre Payeur and David Sénéchal, Phys. Rev. B **83**, 033104 (2011).
- ⁴⁸ Ishiguro T., Yamaji K. and Saito G., Organic Superconductors (Springer-Verlag, New York) 1973.
- ⁴⁹ Tsuda N., Nasu K., Yanese A. and Siratori K., Electronic Conduction in Oxides (Springer-Verlag, Berlin) 1990.
- ⁵⁰ Bishop A. R. and Swanson B. I., Los Alamos Sci., 21 (1993) 133; Fehske H., Kinatader M., Wellein G. and Bishop A. R., Phys. Rev. B, 63 (2001) 245121.
- ⁵¹ Hase M., Terasaki I. and Uchinokura K., Phys. Rev. Lett., 70 (1993) 3651.
- ⁵² Sahinur Reja, S. Yarlagadda, and Peter B. Littlewood., Phys. Rev. B 86, 045110 (2012)
- ⁵³ Steven R. White, Phys. Rev. Lett. **69**, 2863 (1992)
- ⁵⁴ Ravindra Pankaj and Sudhakar Yarlagadda, Phys. Rev. B 86 035453 (2012)
- ⁵⁵ A. Ghosh and S. Yarlagadda, Phys. Rev. B 96, 125108 (2017)
- ⁵⁶ I. G. Lang and Yu. A. Firsov, Zh. Eksp. Teor. Fiz. **43**, 1843 (1962) [Sov. Phys. JETP **16**, 1301 (1962)].
- ⁵⁷ Doohee Cho, Yong-Heum Cho, Sang-Wook Cheong, Ki-Seok Kim, and Han Woong Yeom Phys. Rev. B 92, 085132 (2015)
- ⁵⁸ H. Eskes and R. Eder, Phys. Rev. B **54**, 14226 (1996).
- ⁵⁹ B. Ammon, M. Troyer, and H. Tsunetsugu, Phys. Rev. B, **52**, 629 (1995).
- ⁶⁰ A. P. Balachandran, E. Ercolessi, G. Morandi, and A. M. Srivastava, Int. J. Mod. Phys. B, **4**, 2057 (1990).